PERGAMON

Electrochimica Acta 45 (2000) 4553–4557

ELECTROCHIMICA Acta

www.elsevier.nl/locate/electacta

Variation of carboxylate-functionalized cyanine dyes to produce efficient spectral sensitization of nanocrystalline solar cells

A. Ehret, L. Stuhl, M.T. Spitler *

ChemMotif Inc., PMB 211, Concord, MA 01742-2411, USA

Received 6 December 1999

Abstract

The sensitizing properties of cyanine dyes in dye-sensitized nanocrystalline TiO_2 solar cells are shown to be controlled by the character of the carboxyl functions used to attach the molecules to the surface. These tether functions affect the degree of aggregation of the subject cyanine dyes attached to TiO_2 as well as the short circuit photocurrents they produce in these solar cells. Use of two carbons, acetic acid linkages, on the dye results in performance in a sensitized solar cell comparable with a control ruthenium complex, in contrast to the greatly diminished performance of dyes with longer, methylbenzoic acid linkages. © 2000 Elsevier Science Ltd. All rights reserved.

Keywords: Titanium dioxide; Cyanine dyes; Nanocrystalline solar cells

Dye-sensitized solar cells have been shown to operate with power conversions of up to 10% when nanocrystalline TiO_2 electrodes have been used as a solid substrate and organometallic ruthenium complexes as sensitizers [1]. However, it is necessary to attach the sensitizer to the solid through specific functions on the chromophore. For TiO_2, it is believed that specific sites on the surface, such as Ti(III) atoms, are complexed by these ligand functions to provide a secure link between the sensitizer and solid. Carboxyl and phosphonate groups on the dye have been shown to work well in this role [2,3]. Many variants of Ru(II) chromophores have been explored that have different numbers and locations of these linking functions; the efficacy of the sensitizer has been found to be dependent on these variables [1,2]. A simple Ru(II)(2,2′-bipyridyl-4,4′dicarboxylate)$_3^{4-}$ complex, for example, does not perform as well as Ru(II)(2,2′-bipyridyl-4,4′dicarboxylate)$_2$Cl$_2^{4-}$, which in turn, is less effective than the standard Ru(II)(2,2′-bipyridyl-4,4′dicarboxylate)$_2$-(NCS)$_2^{4-}$ (N3) complex.

Organic dyes have also been examined as sensitizers in dye-sensitized solar cells [4–6]. Organic dyes have been complexed with cyclodextrins to bind well to nanocrystalline TiO_2, but function poorly in a solar cell [4]. A merocyanine dye with a single carboxyl linkage has been shown to form J-aggregates on nanocrystalline solids, but its ability to sensitize a solar cell was reported to be poor [5]. Blue-shifted H-aggregates of organic dyes can be formed in many ways on a nanocrystalline surface, but have not exhibited the performance in dye-sensitized solar cells that is comparable with that of N3 [6].

In this study we demonstrate how the spectral characteristics of an efficient organic sensitizer in dye-sensitized solar cells can be controlled through placement and manipulation of the chelating carboxyl linkages on the chromophore. The primary observation is that a

* Corresponding author.

PII: S0013-4686(00)00606-X

minimum of two carboxyl links are required for a dye to perform well in these solar cells.

Cyanine dyes are used for this purpose and are synthesized with different carboxylic acid functions for linking the dye to the TiO_2 surface. The different tethering linkages of these organic dyes serve to constrain the possible orientation of the dyes on the surface. In some cases only monomeric forms of the dyes are allowed. In others, only aggregated forms of the dyes result.

These dyes are used in dye-sensitized solar cells made with nanocrystalline TiO_2. Their sensitizing characteristics in these cells are characterized through the measurement of short circuit photocurrents, open circuit voltages, and photocurrent action spectra. In comparison, the performance of N3 is used as a control. Short circuit photocurrents and open circuit photovoltages from solar cells made with these dyes are comparable with those from N3 control cells, demonstrating that organic dyestuffs can function well in this application.

1. Experimental

The structures of the dyes used in this study are given in Fig. 1.

The trimethine dyes were synthesized through the following procedure.

1.1. 2,2′-(dipropylcarboxy)-9-ethyl-thiacarbocyanine bromide (G2)

One g (3.31 mmol) of *N*-(3-propanoic acid) 2-methylbenzthiazolium bromide was added to 45 ml of acetonitrile along with 4000 mg (2.27 mmol) of triethylorthoproprionate. Triethylamine (0.46 g) (4.50 mmol) was added to the stirred acetonitrile solution. An immediate yellow precipitate was formed. The solution was heated to reflux and held for 1 h and cooled in an ice bath. The solid precipitate was filtered and recrystallized out of ethanol. Yield, 900 mg (72%). The resulting dye gave one spot in TLC analyses and an extinction coefficient of 9.5×10^5 cm^2 mmol^{-1} at 546 nm in ethanol.

Pentamethine dyes were synthesized through the following procedure.

1.2. 2,2′-(dipropylcarboxy)thiadicarbocyanine PF_6 (R4)

The synthesis of R4 was based on the procedure in the second example of [7]. In a 50 ml round bottom flask with magnetic stirring bar and reflux condenser fitted with an N_2 inlet was placed 1.055 g (3.51 mmol) of *N*-(2-propanoic acid)-2-methylbenzothiazolium bromide, 0.288 ml (1.75 mmol) malondialdehyde bisdimethylacetal (Aldrich), and 4.0 ml pyridine. This mixture was stirred under N_2 and heated to reflux for 15 min, and the reaction mixture was allowed to cool under N_2. This dye can be isolated as its PF_6^- salt by adding NH_4PF_6 and HCl to get a powder that can be recrystallized from hot acetone/water.

The synthesis of the quaternary amine salts necessary for dye synthesis followed known procedures in which the reagents were added to pressure vessels and heated for 1 h in an oil bath at temperatures exceeding 100°C.

The TiO_2 preparation was made using titanium isopropoxide and nitric acid after the manner of Grätzel [1,8]. The TiO_2 fluid was spread on 1 in. square conductive SnO_2 glass using wire wound Mayer rods to control the coating thickness. Following coating, the samples were allowed to dry and then heated to 450°C in 30 min and held there for a further 30 min. At a 15% solid level in the coating solution, the final solid thickness was nominally 4.0 μm. This final thickness was confirmed with a Dektak profilometer.

Solar cells were made with these dyed nanocrystalline layers by mating them with another 8 Ω in. square SnO_2 element and sealing with low temperature, hot melt glue, leaving apertures for insertion of electrolyte. The standard electrolyte composition of 0.50 M NaI/0.05 M I_2 in acetonitrile was used. No attempts were made to optimize these solar cells because this was not

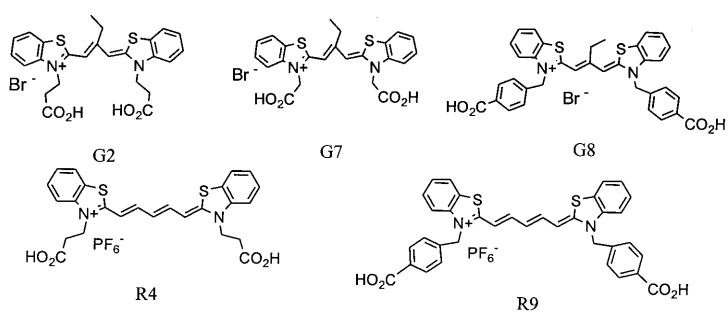

Fig. 1. These structures show the location and nature of the two carboxylic acid functions through which the dyes attach themselves to the nanocrystalline surface.

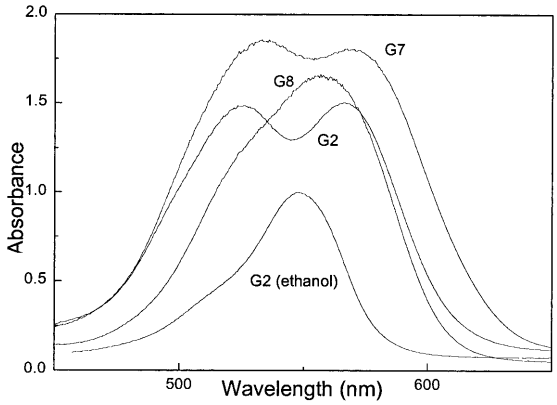

Fig. 2. The absorption spectrum of G2 in solution is contrasted with the spectra of G2, G7, and G8 attached onto 4-μm-thick films of nanocrystalline TiO_2. The dyes were attached to the solid from a dry ethanol solution.

the goal of this study. For example, the colloidal TiO_2 material prior to coating was not sonicated. As a control solar cell, a 10 nm thick N3 sensitized solar cell was made. Its power conversion was estimated at 4.5–5%.

A 250 W tungsten light source provided the light for exposure. The beam was passed through a water filter and a 420-nm cut-off filter. The power incident on the sample was measured with a calibrated silicon photodiode and estimated to be 110 mW cm^{-2}. Compared with a xenon lamp, the spectral distribution of this photon flux is low in the blue end of the spectrum where N3 absorbs and slightly higher in the red end. The current–voltage curves were measured using an electronic instrument built in-house. The electrolyte was added to the cell prior to exposure and allowed to sit for several min before exposure and measurement.

Absorption spectra of the dyed TiO_2 layers were made with an AVIV UV/VIS spectrophotometer. Action spectra were taken with the solar cells in short circuit configuration. An Acton Research Corporation scanning monochromator was used with the 250 W tungsten light source to provide the wavelength dependent illumination. The monochromator bandwidth was set at 10 nm. The action spectra were corrected for variations in photon flux with wavelength.

2. Result

2.1. Absorption spectra of dyes on TiO_2

The absorption spectra of dyes G2, G7, and G8 on nanocrystalline TiO_2 are shown in Fig. 2. The dyes were attached to the nanocrystalline TiO_2 layers through immersion of the solid in dry ethanol solutions of the dye. The dye solutions ranged in concentration from 1 to 5×10^{-5} M in concentration. Immersion time for this series of dye experiments was 2 h. It should be noted that forms of these dyes with only one attached carboxyl group did not adhere to the surface, and could be washed off easily with ethanol.

The spectra of the attached dye can be compared with that of monomeric G2 in ethanol, which is also given in Fig. 2 and is superimposable on the solution spectrum of G7 and G8, which are not shown. The spectrum of the TiO_2 attached G8 is most like that of the solution, showing a red shift of some 10 nm for both the main peak and the blue-shifted vibronic shoulder [9]. This contrasts with the twin peaked spectra of G2 and G7 which are attached closer to the surface than allowed by the methylbenzoic acid linkage of G8. The blue-shifted peak of the G2 and G7 spectra can be attributed to aggregates of the dyes [10]; the two maxima in the spectrum imply the presence of a heterogeneous mixture of monomer and aggregate on the surface. On the other hand, the bulky methylbenzoic acid function of G8 apparently serves to preclude the dye–dye interaction that produces aggregates.

The pentamethine dyes R4 and R9 illustrate other aspects of aggregate formation when attached to nanocrystalline TiO_2. When the solid is immersed in an ethanolic solution of these dyes, aggregates are formed on the surface. The spectrum of R4 on TiO_2 that is shown in Fig. 3 reveals a broad featureless absorption at about 600 nm with a smaller red-shifted peak. Qualitatively, this is similar to the spectra of G2 and G7 in Fig. 3, except that the blue-shifted peak has come to dominate the spectrum. This broad and featureless aggregate peak is heterogeneous in nature and represents the absorption of different kinds of blue-shifted H-aggregates on the surface of the TiO_2. [11] The aggregate absorption is about 100 nm in width and is broader than the absorption of any of the 'G' dyes in Fig. 2. The ethyl-carboxy attachment function appears flexible enough to allow many different geometric configurations for dye–dye interactions, including that of the monomer as its longer wavelength shoulder. In contrast, the spectrum of R9 in Fig. 3 shows a peak with a sharper edge in the blue, with only a minimal peak evident in the red. The sharper peak to the blue is evidence of a greater number of more extended H-aggregates than R4, so much so that the monomeric contribution is effectively suppressed.

To illustrate the difference between monomer and H-aggregated dimer for a trimethine cyanine dye, the spectrum of G2 in ethanol is contrasted in Fig. 4 with that of G2 in an ethanol/water mixture. This monomer/dimer equilibrium for thiacarbocyanine dyes has been the subject of previous study [10]. It can be seen that the absorption of an H-aggregated dimer of a cyanine dye has a sharp and well-defined spectrum, unlike that

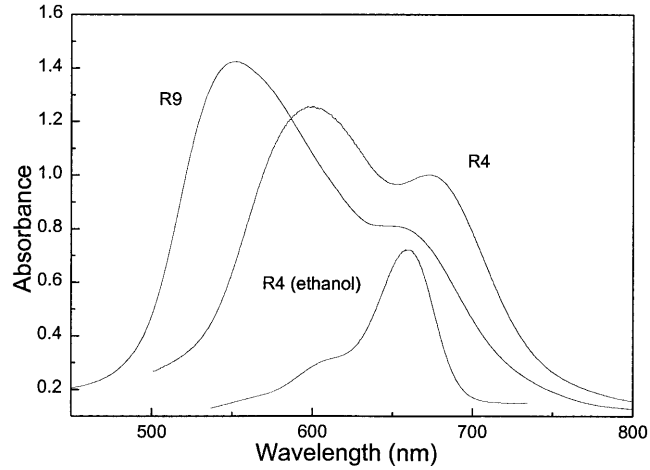

Fig. 3. The absorption spectrum of R4 in solution is contrasted with the spectra of R4 and R9 attached onto 4-μm-thick films of nanocrystalline TiO_2. The dyes were attached to the solid from a dry ethanol solution.

of the R4 absorption of Fig. 3, but much like the blue portion of the spectrum of G2 in Fig. 2. It is evident that the spectrum of the G2 on TiO_2, which is also given in Fig. 4, can be deconvolved as a combination of monomer and dimer forms on the surface. It is a unique situation to find that the aggregation of a dye on surfaces is limited to a dimer; the typical behavior is that of the 'R' spectra of Fig. 3 where the presence of a great number of extended dimers is evident.

2.2. Performance in dye-sensitized solar cells

The action spectra of these dyes in a dye-sensitized solar cell match their absorption spectra. We show this in Fig. 5, where the action spectra of G2 and R4 are compared with their absorption spectrum. The congruence is within experimental accuracy. This implies a sensitization of the solar cell from all forms of the dye on the surface, aggregated or not, with equal yields for charge injection and separation.

A range of short circuit photocurrents produced by these dyes in a 4-μm-thick solar cell are listed in Table 1, along with a typical value of the open circuit photocurrents. Fill factors ranged between 60 and 80%.

3. Discussion

It is evident that short circuit photocurrents for the dyes of this work can be high. Although those of R4, G8 and R9 are low, those of G7 are comparable with the N3 chromophore that is commonly used as a high performance sensitizer in dye-sensitized solar cells. In contrast to previous study with organic dyes as sensitizers in dye-sensitized solar cells, this study shows that a variety of suitable organic sensitizers can be found [4–6]. With this limited selection of dyes studied, the primary innovation appears to be in the use of two linkages for attachment. This performance as sensitizers in a solar cell is not unexpected. These cyanine chromophores are known to be effective sensitizers in silver halide systems [11].

One advantageous characteristic of these dyes is their high oscillator strength *f*. For example, it has been determined [9] that *f* for 3,3′ diethylthiacarbocyanine, which is the basic chromophore for G2, G7, and G8, is 1.02. This contrasts with the *f* value of 0.140 calculated for $Ru(II)(bipyridyl)_3^{2+}$ using an extinction coefficient of 14 000 (at 450 nm in ethanol) and the *f* value of 0.197 calculated for N3 using an extinction coefficient of 14 000 (534 nm in ethanol). Therefore, much less of

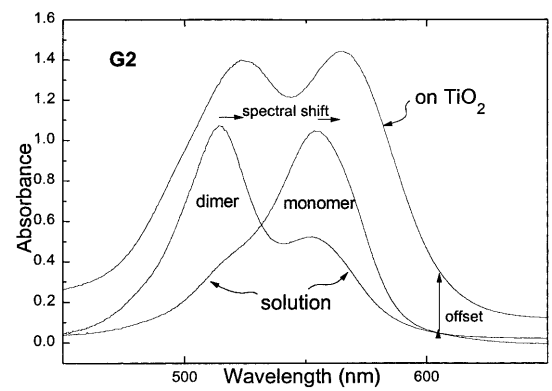

Fig. 4. Monomer and dimer forms of G2 in solution yield distinctly different spectra. The dimerization of G2 in ethanol was induced through addition of water. It can be seen that the spectrum of G2 on TiO_2 contains contributions from both forms of the dye and is red-shifted by the 10–15 nm expected for a dye on a solid surface. The spectrum is offset for clarity.

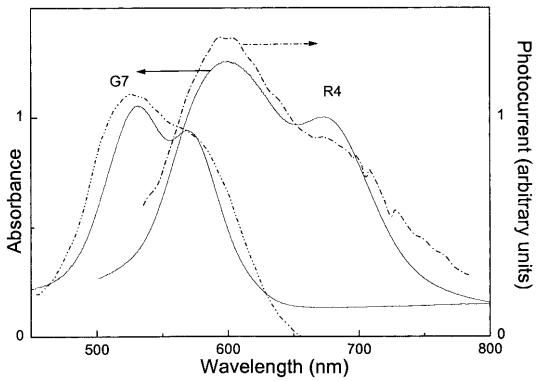

Fig. 5. In solid lines are given the absorbances of nanocrystalline layers dyed with G7 and R4. When these layers are inserted into a solar cell, the absorption spectra are found to be good predictors of the action spectra for the short circuit photocurrent of these solar cells, which are given as dashed lines.

Table 1
Typical short circuit photocurrents (I_{ss}) and open circuit voltages (V_{oc}) for 4.0 μm layers

	I_{ss} (mA cm^{-2})	V_{oc} (mV)
G2	3.2–3.4	465
G7	5.9–6.4	450
G8	1.4–1.8	390
R4	1.8–2.1	380
R9	1.7–1.9	400
N3	5.4–6.3	440

the organic cyanine dye is necessary to equal the absorption of the N3 dye on the TiO_2.

However large the f for the cyanine dyes, their absorption is narrowly confined in spectral width. Therefore, it will be necessary to make combinations of several dyes to cover the spectrum effectively. In this case, it will be necessary to control the spectral components of the sensitizer. It is evident that these tether manipulations can provide the necessary control. They can be used to induce a large, broad aggregation, as seen for R9 in Fig. 3, or much narrower monomer absorption, as is seen for G8 in Fig. 2. With the action spectrum of the dye mapping onto its absorption spectrum in a one-to-one correlation, as is seen in Fig. 5, it is easy to assess the spectral features of the various chromophores, even before insertion into a nanocrystalline solar cell.

There are secondary effects of the manipulation afforded by the attachment function. One is the effect of aggregation on the yield for photocurrent production by the sensitizer. Electron transfer to the TiO_2 is in competition with the internal relaxation processes of the dye, some of which lead to relaxation all of the way to the ground states. The large variation in aggregate configurations afforded by the surface provides a large variation in the rates of relaxation of the excited dye aggregates and therefore a variation in the yield for the electron transfer process. This depends, of course, on the actual rate constant for electron transfer for the specific aggregate of interest, which can be $> 10^{14}$ s^{-1} [12,13] relative to the rates for these internal conversion processes.

Another is the influence of the tether length on electron transfer rate constants. This is an unexplored area in spectral sensitization of solids. Yet another effect is the strength of the linkage function as an acid. The betaine anion linkage of G7 is certainly a much stronger ligand than the methyl-benzoic acid anion of G8. Therefore, they may be able to chelate Ti(III) sites on the surface that the G8 could not. It creates the situation where the location of the attachment will depend on the character of the sensitizer as well as on the treatment of the surface.

Acknowledgements

This study was supported by the U.S. Department of Energy under Contract 98ER82552.

References

[1] M.K. Nazeeruddin, A. Kay, I. Rodicio, R. Humphry-Baker, E. Muller, P. Liska, N. Vlachopoulos, M. Grätzel, J. Am. Chem. Soc. 115 (1993) 6382.
[2] US Patent 5,463,057.
[3] S.G. Yan, J.T. Hupp, J. Phys. Chem. B 100 (1996) 6867.
[4] I. Willner, Y. Eichen, B. Willner, Res. Chem. Intermed. 20 (1994) 681.
[5] F. Neusch, J.E. Moser, V. Shklover, M. Grätzel, J. Am. Chem. Soc. 118 (1996) 5420.
[6] A.C. Khazraji, S. Hotchandani, S. Das, P.V. Kamat, J. Phys. Chem. B 103 (1999) 4693.
[7] US Patent 5,488,114.
[8] US Patent 5,350,644.
[9] W. West, A.L. Geddes, J. Phys. Chem. 68 (1964) 837.
[10] W. West, S. Pierce, J. Phys. Chem. 69 (1894) 1965.
[11] W. West, P.B. Gilman, in: T.H. James (Ed.), Theory of the Photographic Process, forth ed., MacMillan, New York, 1977.
[12] T. Hannapel, B. Burfeindt, W. Storck, F. Willig, J. Phys. Chem. B 101 (1997) 6799.
[13] S. Ferrere, B.A. Gregg, J. Am. Chem. Soc. 120 (1998) 843.